Initial results from the Tokapole-II poloidal divertor device

1979 Nucl. Fusion 19 1509

(http://iopscience.iop.org/0029-5515/19/11/010)

INITIAL RESULTS FROM THE TOKAPOLE-II POLOIDAL DIVERTOR DEVICE

A.P. BIDDLE, R.N. DEXTER, R.J. GROEBNER, D.J. HOLLY,
B. LIPSCHULTZ, M.W. PHILLIPS, S.C. PRAGER, J.C. SPROTT
University of Wisconsin, Madison, Wisconsin,
United States of America

ABSTRACT. The latest in a series of internal-ring devices, called Tokapole II, has recently begun operation at the University of Wisconsin. Its purpose is to permit the study of the production and confinement of hot, dense plasmas in either a toroidal octupole (with or without toroidal field) or a tokamak with a four-node poloidal divertor. The characteristics of the device and the results of its initial operation are described here. Quantitative measurements of impurity concentration and radiated power have been made. Poloidal divertor equilibria of square and dee shapes have been produced, and an axisymmetric instability has been observed with the inverse dee. Electron cyclotron resonance heating is used to initiate the breakdown near the axis and to control the initial influx of impurities. A 2-MW RF source at the second harmonic of the ion cyclotron frequency is available and has been used to double the ion temperature when operated at low power with an unoptimized antenna. Initial results of operation as a pure octupole with poloidal Ohmic heating suggest a tokamak-like scaling of density ($n \propto B_p$) and confinement time ($\tau \propto n$).

1. INTRODUCTION

Internal-ring devices (multipoles, spherators, levitrons, and surmacs) have a long and impressive history of contributions to the understanding of magnetically-confined, toroidal plasmas. Most of the experiments have used relatively cold (few eV), low-density ($10^9 - 10^{12}$ cm^{-3}) plasmas, not out of necessity, however, but rather as an experimental convenience. With the progress in heating and impurity control in tokamaks and the renewed interest in internal-ring devices as advanced fuel reactors [1] and as poloidal divertors for tokamaks, it seemed timely to construct a new internal-ring device specifically to produce and confine hot (few hundred eV), dense (10^{13} cm^{-3}) plasmas. The device, called Tokapole II, is basically an octupole with a relatively strong (up to 10 kG) toroidal field. By controlling the shape and timing of the octupole and toroidal fields, the device can be operated as an octupole (with or without toroidal field), or as a tokamak with a four-node poloidal divertor. Poloidal divertor configurations with square or dee-shaped cross-sections can be produced by adjusting the positions of the internal rings. Plasma in the divertor region can be retained or suppressed by use of a retractable scrape-off plate. The octupole case can be studied with or without Ohmic heating. The versatility of the device allows a direct comparison of a wide variety of magnetic configurations in a device of the same size, field strength, wall cleanliness, etc. This paper will describe the device and initial measurements of the plasma characteristics, with particular emphasis on its operation as a tokamak with a poloidal divertor. Studies of electron cyclotron resonance breakdown and high-power RF heating at the second harmonic of the ion cyclotron frequency will be discussed. Initial results of density and energy confinement time scaling for the pure octupole with poloidal Ohmic heating will also be given.

2. DEVICE DESCRIPTION

The Tokapole II device consists of a 50-cm major radius, 44 X 44 cm square cross-section, 3 cm thick, aluminium, toroidal vacuum vessel which is linked by an 0.15-V · s iron transformer core as shown in Fig.1. The vacuum chamber walls have a field penetration time of about 15 ms, thus ensuring a high degree of magnetic symmetry for the field pulse lengths used. This magnetic symmetry was preserved by machining the vacuum tank to a high precision (0.5 mm) and paying careful attention to the placement of the toroidal and poloidal field primary windings in the vicinity of the toroidal and poloidal voltage gaps.

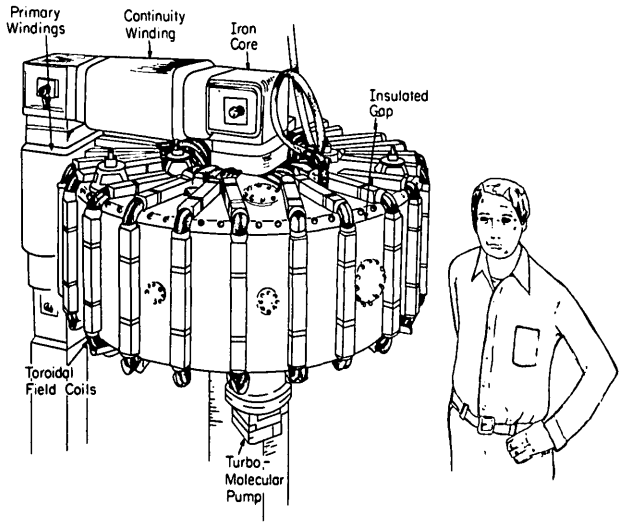

FIG.1. The Tokapole II device.

A total of 42 ports was provided to facilitate diagnostic access, and the ports were arranged wherever possible in pairs on the top and bottom so as to preserve symmetry about the horizontal midplane. The perturbations caused by the larger (19-cm-diameter) pump ports are minimized by the use of 55% transparent copper plugs which have the same average resistivity as the aluminium walls.

The octupole field is produced by four, 5-cm-diameter, solid-copper rings which encircle the iron core and can carry a total peak current of up to 700 kA. The rings were machined to a high tolerance (0.13 mm) and polished. The rings are positioned carefully near the corners of the vacuum vessel so that the three field nulls coalesce into a single octupole null near the minor axis as shown in Fig.2.

Experiments on an earlier device [2], Tokapole I, which was operated as an octupole (four rings), a quadrupole (two rings), and a tokamak (no rings) indicated the difficulty of driving toroidal plasma currents in a low-order field null, as shown in Fig.3. Additionally, it is interesting to note that the toroidal current is proportional to voltage in the tokamak case but proportional to the square of the voltage in the Ohmically heated multipoles.

Each ring is supported by three beryllium-copper rods which are threaded to allow a vertical adjustment of ± 5 mm of each ring position. The total support area of 133 cm^2 limits the confinement time of 100-eV ions in the divertor region to about 1.5 ms. Retractable divertor scrape-off plates with a total area of 535 cm^2 (each side) are also available. The rings are electrically insulated from the vacuum chamber and can be biased up to 10 kV. A 90-kJ capacitor bank, which can produce up to 125 V across the poloidal gap, is used to excite the poloidal field.

The toroidal field winding consists of 96 turns of AWG 4/0 welding cable (1.17 cm diameter) and is secured to the vacuum chamber by 24 sets of aluminium channels as shown in Fig.1. The mechanical

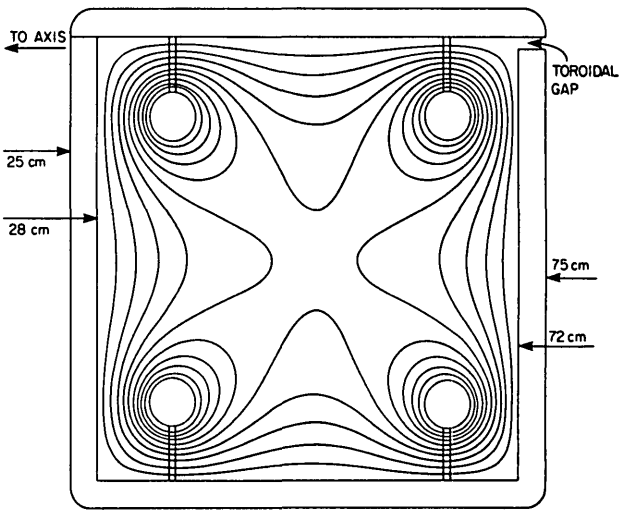

FIG.2. Poloidal magnetic flux plot in the absence of plasma currents.

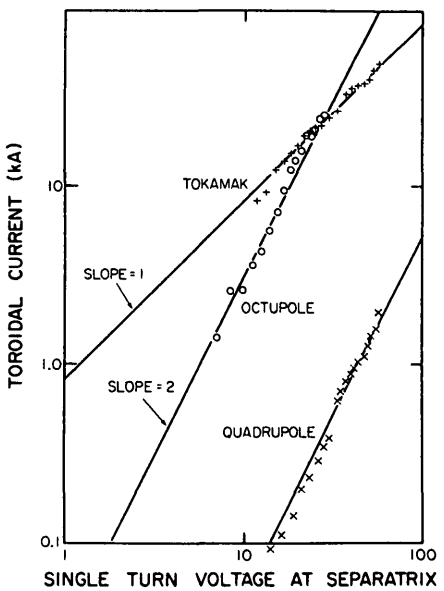

FIG.3. Toroidal current as a function of loop voltage for Tokapole I with four rings (octupole), two rings (quadrupole), and no rings (tokamak).

TABLE I. SUMMARY OF DEVICE CHARACTERISTICS

Major radius: 50 cm
Minor cross-section: 44×44 cm^2
Toroid walls: aluminium, 3 cm thick with poloidal and toroidal insulated gaps
Vacuum volume: 600 litres
Vacuum surface area: 6 m^2
Number of internal rings: 4 (copper, 5 cm diameter, supported at 3 points)
Ports: 2 – 19 cm diam., 5 – 11.5 cm diam., 22 – 4 cm diam., 13 – 0.6 cm diam.
B_T on axis: 3.7 kG (typical), 10 kG (maximum)
L/R time of B_T: 20 ms
Ohmic voltage: 45 V (typical), 125 V (maximum)
Poloidal flux: 0.06 W (typical), 0.15 W (maximum)
Available energy (poloidal + toroidal fields): 505 kJ (5 kV capacitors)
Base vacuum: 3×10^{-8} torr
Pumping system: 1500 litre $\cdot$ s^{-1} turbomolecular pump 1200 litre $\cdot$ s^{-1}, 10 K cryopump
Pre-ionization: 10 kW, 8.8 GHz (10 kW, 16.0 GHz also available)

strength is sufficient to permit toroidal fields of up to 10 kG on axis, but the existing 415-kJ capacitor bank limits the field to 9 kG. A peak field on axis of $\sim$ 3.7 kG was used for most of the experiments described here. Both the toroidal and poloidal fields can be crowbarred with a decay time of $\sim$ 20 ms.

A base vacuum of $\sim 3 \times 10^{-8}$ torr is achieved with a 1500-litre $\cdot$ s^{-1} turbomolecular pump and a 1200-litre $\cdot$ s^{-1} 10 K cryopump. All vacuum seals are viton, but care is taken to ensure that the only insulators exposed to the plasma are ceramic. Provisions were incorporated for baking the entire machine to 150°C, but so far the bake has been limited to 70°C. A residual gas analyser typically shows water to be the dominant impurity. Discharge cleaning is accomplished by pulsing the toroidal field to about 1 kG every two seconds and ringing the poloidal gap with a decaying sine wave of about 50 V and a frequency of about 3 kHz.

A more detailed description of the device is available elsewhere [3]. Table I summarizes the main characteristics of the device.

3. DIAGNOSTICS

Since the internal rings and plasma both link the Ohmic-heating transformer, the measurements of the plasma loop voltage and current are not straightforward. Spatial toroidal electric field profiles are directly obtained by measuring the time-varying poloidal magnetic flux within toroidal loops. Axisymmetry enables this to be done with a small rectangular loop of wire (0.3 cm width in toroidal direction) inserted along the midcylinder to the given radius. Spatial profiles of the toroidal current density are obtained with a small Rogowskii coil (3 cm diameter) or inferred from experimentally measured magnetic-flux plots. A large square cross-section Rogowskii coil can be inserted into the plasma to measure the plasma current flowing in the central channel (inside the separatrix). When in place, the four corners of this coil nearly touch the internal rings. Also, an appropriate circuit model, including the plasma (assumed localized near the minor axis) and the rings, allows us to infer the plasma current by measurement of the poloidal gap voltage and the Ohmic-heating primary current. Electron density is measured with Langmuir probes and a 40 GHz phase-shift microwave interferometer. The interferometer signal is cut off at the maximum density.

Spectroscopic diagnostics include a 1/2-m Jarrell-Ash monochromator, a 1/2-m Seya-Namioka vacuum ultraviolet (VUV) spectrometer, a 1-m Seya VUV monochromator, and a variety of filters and detectors. The 1/2-m Seya is equipped with a phosphor-coated microchannel plate so that we can obtain a panoramic view of the spectral region from 400 – 1300 Å in one shot. This output can be photographed or displayed on a television screen by a gated storage vidicon. The 1-m Seya has been absolutely calibrated and is used to measure impurity-line-radiated power. An absolute calibration for the 1/2-m Seya has been inferred from power measurements with the 1-m instrument.

Ion temperature (T_i) is determined from the Doppler broadening of visible lines of impurity ions and from the He II 4686 Å line. Electron temperature (T_e) is determined with the aid of a computer code

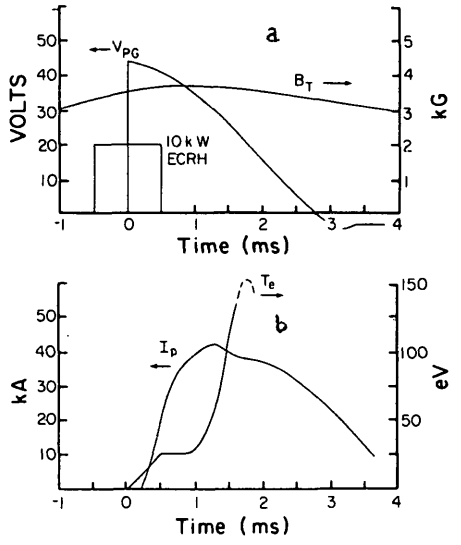

FIG. 4. Time sequence of typical discharge.

which models the observed ionization state sequence of O III through O VI. This technique has been described elsewhere [4].

4. DISCHARGE CHARACTERISTICS

Figure 4a indicates the timing of the fields and pre-ionization for a typical tokamak discharge. A fast piezoelectric valve is used to fill the machine with about 3×10^{-4} torr of hydrogen. About 12.7 ms later, the toroidal field is triggered and is crowbarred when it reaches its peak field strength. Shortly before peak field, a 1-ms pulse of 10-kW, 8.8-GHz microwaves is used as pre-ionization. The Ohmic-heating voltage, which is sinusoidal in time with a quarter-period of 2.8 ms, is triggered during the pre-ionization pulse. The Ohmic-heating primary current can be crowbarred at its peak value.

Figure 4b displays a plasma current (I_p) trace. This yields a peak current of about 40 kA, while the Rogowskii loop gives a peak I_p of about 20 kA, which indicates that about half of the total current flows inside the separatrix. The line-averaged T_e, as determined by the method described above, is also shown in Fig. 4b. T_e is low during the formation of the central current channel and rises to 100 eV or more once the current channel has been formed. This spectroscopic measurement of T_e agrees with the conductivity T_e, if $Z_{eff} = 3$. The ion temperature is about 15 eV and is relatively constant during the discharge. Since T_i is obtained from low-Z impurity ions, this technique only approximates the central ion temperature. The peak, spatially averaged, electron density is about 1×10^{13} cm^{-3}.

Spatial-electric-field and current density data show that after the discharge is well formed, the Ohmic input power to the central channel is 100 – 150 kW while the input power to the entire plasma is 200 – 300 kW. With the assumption that the electron density profile is a cosine, the maximum energy confinement time of the central channel is 250 – 300 μs and that of the full plasma is 100 – 150 μs. The Hugill-Sheffield empirical scaling law for energy confinement time [5] predicts $\tau_E \sim 150$ μs for the central current channel. (The minor radius is taken to be 8 cm, the distance from the magnetic axis to the separatrix.) Confinement in the Tokapole configuration is evidently comparable to that of circular cross-section tokamaks.

5. IMPURITY MEASUREMENTS

In an effort to understand the energy loss mechanisms, we have made qualitative and quantitative impurity line radiation measurements. Most of the radiation has been shown to arise from oxygen, carbon, and nitrogen (associated with vacuum leaks) with lesser amounts from copper and aluminium. Typical impurity concentrations are shown in Table II.

TABLE II. TYPICAL IMPURITY CONCENTRATIONS

Impurity	Density
Oxygen	3×10^{11} cm^{-3}
Nitrogen	2×10^{11} cm^{-3}
Carbon	5×10^{10} cm^{-3}

The densities of the metal impurities have not been determined. From the spectroscopic impurity density measurements, Z_{eff} is estimated to be $\sim 2.5 - 3.5$.

The radiated power from the full plasma in the 400 – 1300 Å region is 35 – 70 kW. Measurements with VUV-transmitting broadband filters and an appropriate detector show that the power radiated at

shorter wavelengths is insignificant. With the exception of C IV, no known important resonance lines lie at wavelengths longer than 1300 Å. Thus, the data indicate that line radiation is not more than about 15 – 30% of the Ohmic input power and that line radiation is not the dominant energy loss mechanism.

Spatial observations show that there are marked poloidal asymmetries in the emission of impurity radiation. In particular, low-ionization states of impurities often radiate intensely near one or more of the internal rings. Evidently, the rings are an important impurity source, but it is not yet clear whether or not they are the primary impurity source. It is likely that impurities diffusing from the rings tend to form shells in the vicinity of the separatrix. In some cases, chordal observations of the soft-X-ray radiation (40 – 210 Å) have been consistent with the assumption that the highly stripped impurities are localized in a shell near the separatrix.

6. EQUILIBRIUM AND STABILITY OF A POLOIDAL DIVERTOR CONFIGURATION

Divertor configurations are becoming more important as solutions to the impurity problems now besetting tokamaks. One such configuration is the poloidal divertor where poloidal flux is diverted axisymmetrically and plasma outside the separatrix is scraped off. The poloidal divertor configuration which is by nature non-circular is also advantageous with respect to q-limited and β-limited MHD-modes. However, the non-circular nature of this configuration makes it unstable to axisymmetric displacements (circular plasmas are neutrally stable). The importance of these axisymmetric modes is apparent and has given rise to a fairly large amount of linear theory using the energy principle – mostly for idealized displacements of ideal analytic equilibria and for numerically calculated equilibria using Princeton's stability code (PEST) [6 – 8]. Recently, the non-linear evolution of the instability has been followed by Jardin [9] by the numerical integration of the two-dimensional, axisymmetric, time-dependent, ideal-MHD equation in toroidal geometry. Axisymmetric displacements of dee [10, 11] and elliptical [12, 13] plasmas have been deduced in a few previous experiments from magnetic probes external to the plasma. Plasma shapes and positions have been inferred from equilibrium computer codes using external experimental signals as input.

We have made the first direct experimental observation of the stability to axisymmetric modes of square and inverse-dee shaped equilibria in a 4-null poloidal-divertor configuration [14]. Equilibrium is verified by mapping the flux plot as a function of time, and its stability is determined by studying the evolution of these flux plots. We have found that inverse-dee- and square-shaped equilibria exist and that inverse-dee-shaped equilibria are more unstable than the square equilibria. Growth times for the inverse dee are ~ 1000 poloidal Alfvén times implying that passive stabilization due to the rings and walls has occurred.

As part of the programme to study the equilibrium and stability of poloidal-divertor configurations, an axisymmetric magnetohydrodynamic equilibrium code was written to handle internal ring devices with current-carrying plasmas such as the Tokapole II. This code solves the Grad-Shafranov equation for the poloidal flux, ψ, given pressure and poloidal current as functions of ψ and subject to the proper boundary conditions outside the plasma. The plasma is assumed to be confined in the central region of the torus in a divertor configuration where the boundary of the plasma is one of the separatrices. Since the plasma/vacuum interface must be solved as part of the problem, this is a free-boundary-type of problem. Since these problems are non-linear, it is necessary to use iteration techniques to find the solution. The current in the rings and the plasma is induced inductively so the proper representation of the internal rings is to take their surfaces to be Dirichlet boundaries. Hence, the currents in the rings will be coupled to the plasma providing some degree of wall stabilization.

A sample calculation for one of the standard ring configurations and for typical Tokapole II parameters is shown in Fig.5. The general tendency of the plasma is to lean against the outside rings with the resulting image currents (in the rings and wall) providing a vertical field to keep the plasma centrally located.

Since internal probes may be used as a diagnostic, Tokapole II provides the opportunity to verify first hand the shape and subsequent development of its various equilibrium configurations. Figure 6 shows one such experimentally determined flux plot for roughly the same parameters and ring placement as the sample computer calculation. The values of poloidal flux in this plot were found by integrating measurements of the poloidal magnetic field taken on a 2-cm grid. As can be seen, the agreement is fairly good. Preliminary results have shown that when the plasma outside the separatrix is scraped off, the axisymmetric stability of the equilibrium is unaffected.

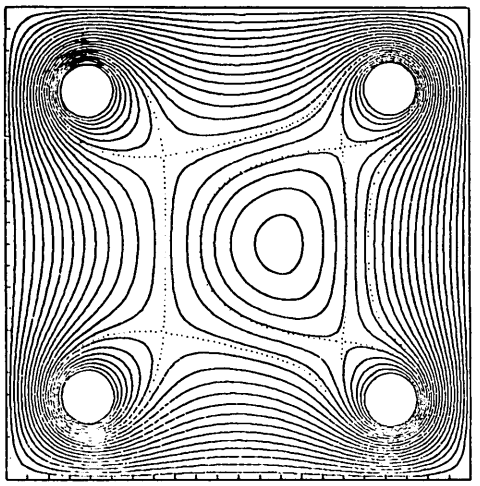

FIG.5. Numerically calculated poloidal flux plot with a plasma current.

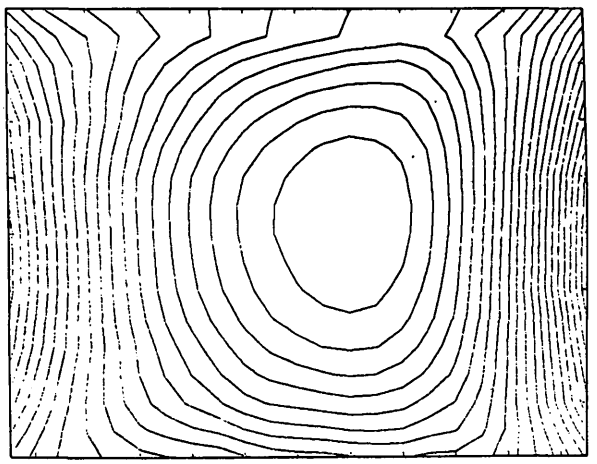

FIG.6. Experimentally measured poloidal flux plot in the region near the magnetic axis.

7. ELECTRON CYCLOTRON RESONANCE BREAKDOWN

Ten kW of 8.8 GHz ECRH is applied before the Ohmic heating begins, as shown in Fig.4. Since at this time the magnetic field is purely toroidal and is roughly constant in time, the ECRH resonance zone is a vertical cylinder. By varying the strength of the toroidal field, the resonance zone can be positioned at different radii. By thus starting the discharge with ECRH, impurity radiation can be reduced by up to about 50% compared to an Ohmic discharge without ECRH pre-ionization.

Langmuir probe traces (Fig.7) taken with no poloidal (Ohmic heating) field show that ECRH results in a plasma profile which peaks at the resonance zone as expected. This is also verified by visible-light photographs of the ECRH plasma. However, when some Ohmic heating is added, Langmuir probe measurements show little difference with and without the pre-ionization (Fig.8). Photographs of the plasma also show no change due to the pre-ionization once the Ohmic-heating power has been applied.

However, the impurity radiation in the VUV, which arises principally from oxygen, carbon, and nitrogen, does show a marked decrease for the first two milliseconds of the discharge when ECRH pre-ionization is used. For the remainder of the discharge, the VUV radiation returned to the level observed in the case with no pre-ionization. The effect of the ECRH pre-ionization on impurity radiation is a function of the position of the ECRH resonance location.

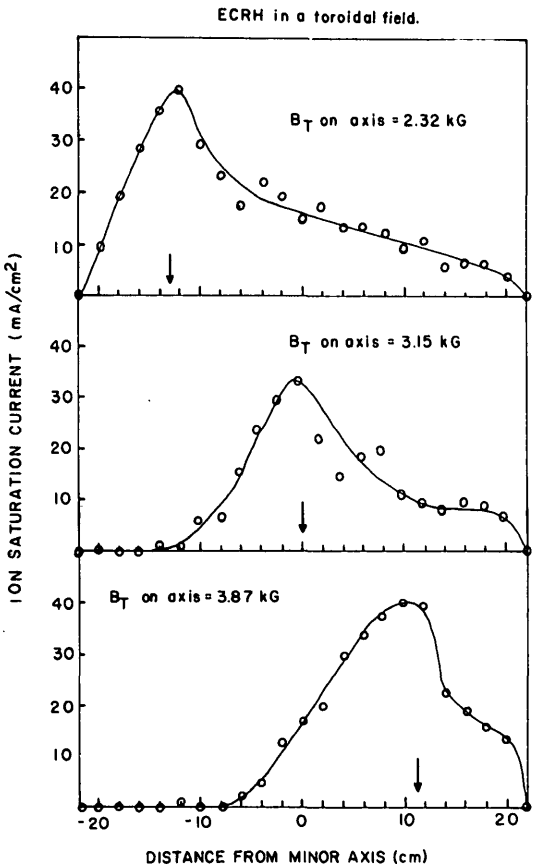

FIG.7. Spatial profiles of ion saturation current for the ECRH pre-ionization plasma for various resonance zone positions. Arrow indicates electron cyclotron resonance zone.

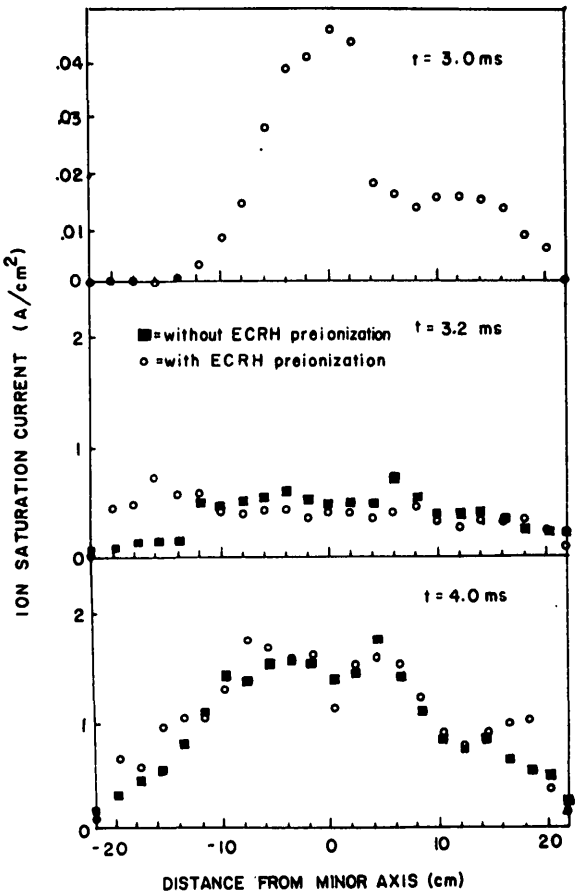

FIG.8. Spatial profiles of ion saturation current just before and at various times after the initiation of the Ohmic discharge with and without ECRH pre-ionization.

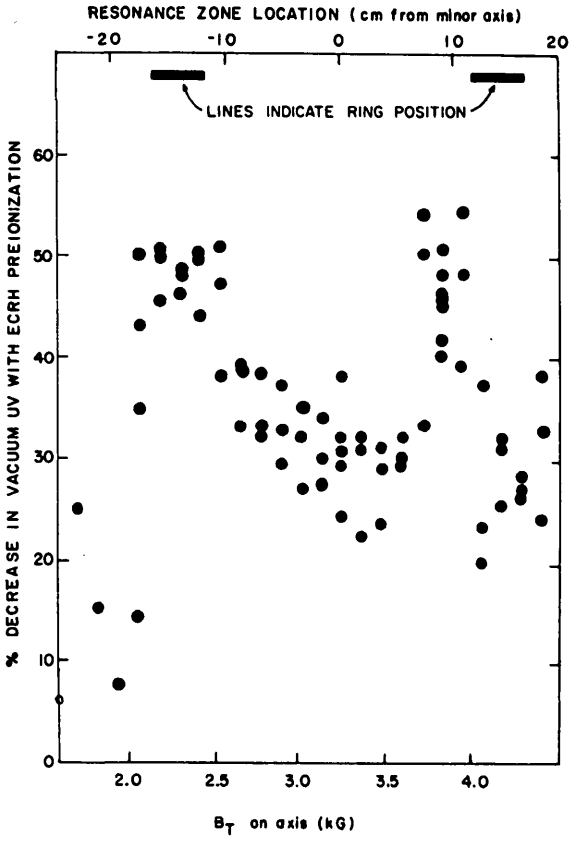

FIG.9. Percentage decrease in VUV radiation as a function of the ECRH resonance zone location.

Figure 9 shows the percent decrease in VUV radiation when ECRH pre-ionization was used, relative to the case with no pre-ionization, as the resonance zone was swept across the machine by varying the toroidal field strength. The effect of the ECRH is to decrease the impurity radiation as much as 50% compared to the no-pre-ionization case. Surprisingly, the effect is most pronounced when the resonance zone intersects the rings.

The intensity of the Cu I radiation line is also much enhanced when the pre-ionization resonance zone intersects the copper rings. This effect persists for the duration of the discharge. Gross plasma parameters, such as the plasma current, are affected much less by the pre-ionization (usually 10% or less). This may be in part due to the rings producing a central current channel with a stable equilibrium, accomplishing the same result as the ECRH pre-ionization. Thus the effect of ECRH pre-ionization might be more dramatic in a tokamak without a poloidal divertor.

8. ION CYCLOTRON RESONANCE HEATING

Tokapole II is providing a unique opportunity for the study of several phases of high-power ICRF heating in a plasma which has a rectangular cross-section and nearly uniform density within the current channel. The 29-cm plasma cross-section is surrounded by a 7.5-cm blanket of reduced density outside the magnetic limiters. As a result, toroidal eigenmodes in the vicinity of the ion cyclotron frequency are few enough to be unambiguously identified and mapped by RF-field probe measurements. The relatively large evanescent region allows detailed studies of wave coupling when the antenna is separated from the dense core of the plasma. Because of the approximately square plasma cross-section, a rectangular rather than cylindrical plasma-filled waveguide model was adopted. Figure 10 shows the two theoretically accessible modes, and Fig.11 shows RF probe measurements of the $\nu = 1$ mode, including the large evanescent region.

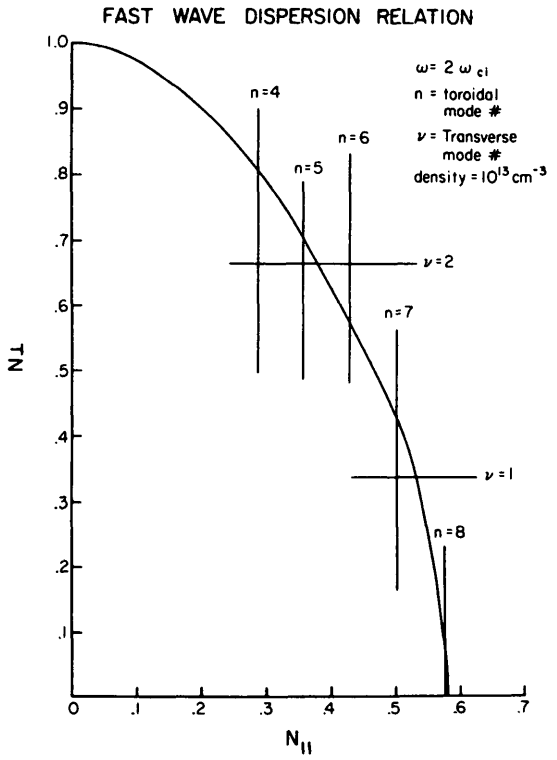

FIG.10. Dispersion relation for the fast magnetosonic wave at $\omega = 2\omega_{ci}$ *in Tokapole II.*

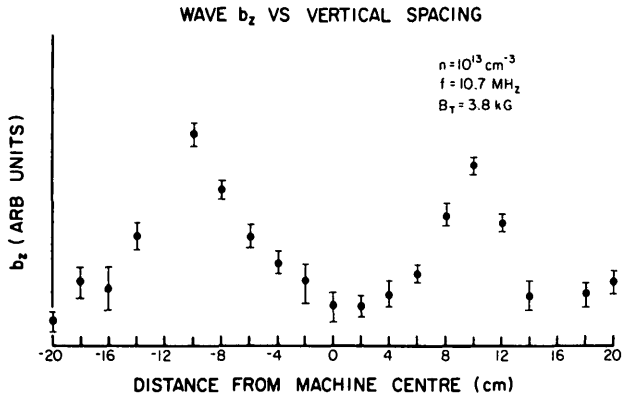

FIG.11. Measured value of the spatial variation of the RF magnetic field showing the radial structure of the toroidal eigenmode.

These studies are being done with a 2-MW self-excited RF-source with a 1.2-ms square pulse length and a temporary antenna located physically outside the vacuum tank and which views the plasma through a 19-cm-diameter ceramic window. For these experiments, one of the copper plugs must be removed from the large ports. As the antenna is also the inductor of the tank circuit, the oscillator frequency tends to track changes in plasma reactance, thereby broadening the modes. Operation at $2\omega_{ci}$ in a hydrogen plasma has doubled the ion temperature as measured by Doppler broadening of the 4686 Å line of doped helium (Fig.12). This represents ~ 10% coupling to the ions, with the balance of the power tentatively identified with plasma edge and tank wall deposition. Impurity line radiation is seen to scale with applied power. However, no disruption of the plasma has resulted from the impurity influx. In fact, a characteristic of the Tokapole II device is that major disruptions which result in complete loss of the plasma do not occur for any of the plasmas which have been examined. This may be due to the stable multipole region which surrounds the toroidal current channel.

Upgrading the launching structure to one whose separation from the plasma is continuously variable and increasing the toroidal field are expected to dramatically increase coupling efficiencies as well as allow heating in an H-D plasma with greatly reduced edge heating. The relatively low poloidal flux is expected to limit maximum ion temperatures, however.

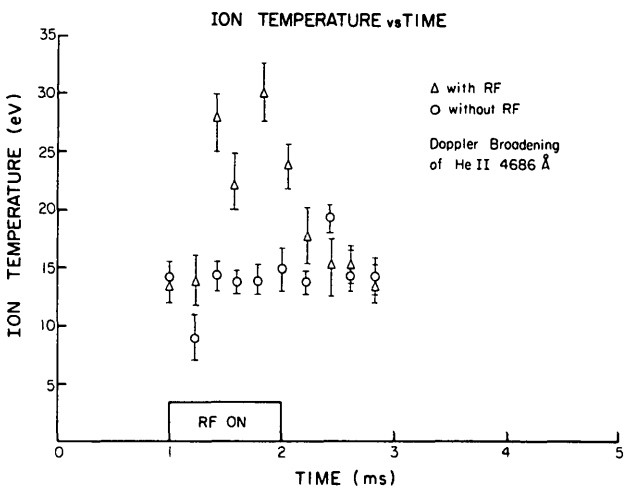

FIG.12. Ion temperature versus time with and without ICRH as determined by Doppler broadening of the He II 4686 Å line.

9. PURE OCTUPOLE OPERATION

Multipoles are of considerable interest as advanced fuel reactors because a stable equilibrium can be obtained without the need for a toroidal field. Furthermore, the poloidal magnetic field has a low average value, and so the synchrotron radiation which would result at the high temperatures needed to burn the advanced fuels (several hundred keV) can be reduced to a tolerable level. However, very little is known about the scaling of energy confinement of hot, dense plasmas in a pure multipole configuration. The Tokapole II has provided an opportunity to extend the extensive measurements at low temperatures and densities into more reactor-like regimes.

To do this, the timing sequence of the magnetic fields is changed somewhat from that shown in Fig.4. The discharge is initiated in a manner similar to that used for the tokamak studies, but after a hot, dense plasma is created, the toroidal field is abruptly ($\sim$ 1 ms) reduced to zero. This abrupt decrease in toroidal field drives current poloidally and produces additional Ohmic heating. Such poloidal Ohmic heating may have distinct advantages over the toroidal Ohmic heating used in tokamaks and stellarators. The resistivity is greatly enhanced (typically a hundredfold) by the strong magnetic mirrors. Additionally, the Krushkal-Shafranov limit presumably does not preclude arbitrarily large values of Ohmic heating.

After the toroidal field has reached zero, one is left with a plasma with parameters similar to those previously described but in a pure octupole field with no Ohmic heating. The subsequent decay of the plasma can then be studied. The first such experiments used a specially shaped Langmuir probe which extends across the bridge region (the narrow region between a ring and the wall shown in Fig.2) so as to volume-average the plasma density.

Figure 13 shows the density measured as described at the end of the poloidal Ohmic heating pulse as a function of the total current in the rings (which is a measure of the poloidal field strength). An approximate linear scaling is observed ($n \propto B_p$) which resembles the scaling of density with toroidal field which is observed in tokamaks. The ion saturation current to the probe is observed to subsequently decay in an approximately exponential manner with a decay time τ which is plotted as a function of initial density in Fig.14. Again, note the approximate linear dependence ($\tau \propto n$) at the higher densities which is characteristic of many tokamak experiments. Since

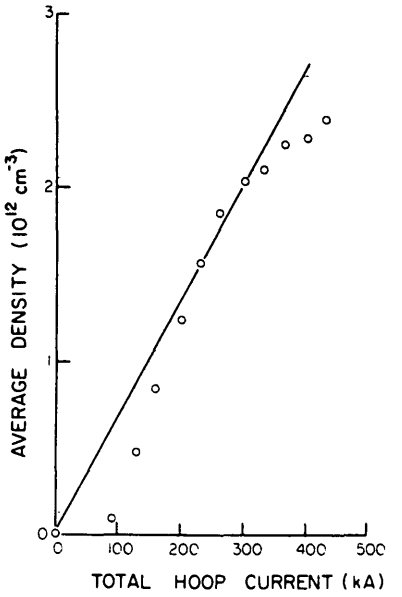

FIG.13. Density as a function of poloidal magnetic field for the pure octupole with poloidal Ohmic heating.

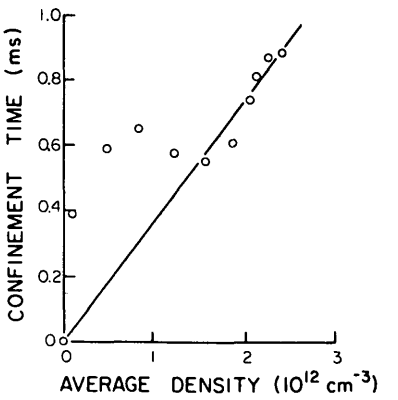

FIG.14. Confinement time versus density for the pure octupole configuration.

the ion saturation current is proportional to $n\sqrt{T_e}$, the measured τ is a mean between the particle and energy confinement times. These results suggest that a multipole with poloidal Ohmic heating enjoys the same favourable scaling as tokamaks.

10. SUMMARY AND CONCLUSIONS

The Tokapole II device is a small, low-field tokamak with a four-node poloidal divertor and the additional flexibility of operating as a pure octupole. Toroidal field and Ohmic heating can be used or not as desired.

The general discharge characteristics agree favourably with those of similar tokamaks. Spectroscopic measurements show that impurity line radiation cannot account for more than ~ 20% of the losses. Divertor configurations of square and inverse-dee shapes can be produced, and the inverse dee is observed to develop an axisymmetric instability in which the magnetic axis moves toward one of the divertor rings on a time scale of ~ 1000 poloidal Alfvén times. The square case appears to be stable. One novel feature of the experiment is the use of ECRH pre-ionization which helps to initiate the Ohmic discharge away from the walls, resulting in a 50% reduction in impurity radiation. A 2-MW ICRH source is available, and has been used to double the ion temperature, but with poor coupling efficiency resulting from the lack of a proper antenna. When operated as a pure octupole, the density and confinement time obey tokamak-like scaling. Future work will include doubling the toroidal field strength and discharge length, increasing the ICRH power coupled to the plasma, studying the stability of the various poloidal divertor configurations at high beta and low q, and determining the scaling and limitations of poloidal Ohmic heating.

ACKNOWLEDGEMENTS

We are grateful to K. Miller, T. Osborne, M. Sengstacke, D. Shepard, and D. Witherspoon for assistance in assembly of the apparatus and some diagnostic measurements. Engineering and technical support was provided by T. Lovell and R. Vallem. This work was supported by the US Department of Energy.

REFERENCES

[1] DAWSON, J., Bull. Am. Phys. Soc. **24** (1979) 42.
[2] DORY, R.A., KERST, D.W., MEADE, D.M., WILSON, W.E., ERICKSON, C.W., Phys. Fluids **9** (1966) 997.
[3] SPROTT, J.C., Small-Toroidal-Device Users (Proc. Meeting Monterey, Cal., May 18, 1978).
[4] EQUIPE TFR, Nucl. Fusion **15** (1975) 1053.
[5] HUGILL, J., SHEFFIELD, J., Nucl. Fusion **18** (1978) 15.
[6] BERRY, L.A., BUSH, C.E., CALLEN, J.D., COLCHIN, R.J., DUNLAP, J.L., et al., in Plasma Physics and Controlled Nuclear Fusion Research (Proc. 6th Int. Conf. Berchtesgaden, 1976) Vol.1, IAEA, Vienna (1977) 49.
[7] BERNARD, C., BERGER, D., GRUBER, R., TROYON, F., Gulf General Atomic Report GA-A1485 (1978).
[8] MANICKAM, J., DALHED, S., DELUCIA, J., GRIMM, R.C., HSIEH, V.Y., JARDIN, S.D., JOHNSON, J.L., OKABAYASHI, M., TODD, A.M.M., WEIMER, K.E., Bull. Am. Phys. Soc. **23** (1978) 897.
[9] JARDIN, S.C., JOHNSON, J.L., GREENE, J.M., GRIMM, R.C., Comput. Phys. **29** (1978) 101.
[10] TOYAMA, H., INOUE, S., ITOH, K., IWAHASHI, A., KANEKO, H., et al., in Plasma Physics and Controlled Nuclear Fusion Research (Proc. 6th Int. Conf. Berchtesgaden, 1976) Vol.1, IAEA, Vienna (1977) 323.
[11] SAKURAI, K., NAKAMURA, K., KUZUSHIMA, T., TANAKA, Y., OKUDA, T., J. Phys. Soc. Jpn **43** (1977) 731.
[12] CIMA, G., ROBINSON, D.C., THOMAS, C.L., WOOTON, A.J., ibid., 335.
[13] WOOTON, A.J., Nucl. Fusion **18** (1978) 1161.
[14] LIPSCHULTZ, B., PRAGER, S.C., OSBORNE, T.H., SPROTT, J.C., PHILLIPS, M., Phys. Rev. Lett. **43** (1979) 36.

(Manuscript received 30 March 1979
Final version received 7 July 1979)